Qubit readout and quantum sensing with pulses of quantum radiation

(article starts on next page)

Qubit readout and quantum sensing with pulses of quantum radiation

Maryam Khanahmadi [1,2,*] and Klaus Mølmer[3,†]

[1]*Department of Microtechnology and Nanoscience, Chalmers University of Technology, 412 96 Gothenburg, Sweden*
[2]*Department of Physics, Institute for Advanced Studies in Basic Sciences, Zanjan 45137, Iran*
[3]*Niels Bohr Institute, University of Copenhagen, Blegdamsvej 17, DK-2100 Copenhagen, Denmark*

Different hypotheses about a quantum system such as the logical state of a qubit or the value of physical interaction parameters can be investigated by the interaction with a probe field. Such fields may be prepared in particularly sensitive quantum states and we demonstrate here the use of quantum trajectories to model the stochastic measurement record and conditional evolution of the state of the quantum system subject to its interaction with a traveling pulse of radiation. Our analysis applies to different measurement strategies and to arbitrary input quantum states of the probe field pulse and it thus permits direct comparison of their metrological advantages. A theoretical lower limit to the mean discrimination error can be calculated in a deterministic manner and we verify that it lies below the average inference error in all our examples.

I. INTRODUCTION

The motivation in quantum optics to study a variety of so-called nonclassical states of light, such as number states, squeezed states, entangled states, and Schödinger cat states has been associated with their use in precision measurement protocols. Very sensitive measurements may thus benefit from the use of probe fields that are prepared in states that change maximally upon the interaction with the object or phenomenon under investigation while displaying minimal variance of the observable measured [1,2]. More general approaches adopt advanced analyses of the information that can be extracted by optimal general measurements on the quantum state [3].

In this article we consider probing of a quantum system by its interaction with an itinerant traveling wave packet of quantum light or microwave photons, see Fig. 1. Propagating quantum states were proposed to mediate quantum state transfer and quantum interactions between stationary physical systems [4–8], but a practical theory for how a single-mode input pulse of quantum radiation interacts with a local quantum system was only presented recently [9–13]. The purpose of the present study is two-fold: On the one hand, we shall extend previous, simplified treatments and provide a description of how the traveling quantum pulse interacts with matter in a fully time-dependent manner, and, on the other hand, we shall present an analysis of the full measurement record from the continuous probing of the radiation field after the interaction with the system of interest.

A nonlinear scatterer generally produces a multimode output field which does not have a manageable quantum state description in terms of a state vector or density matrix. But, in [11,12], it was shown that it is possible to calculate the dynamics of the scatterer by a cascaded systems master equation where the output field is treated as a loss. We shall incorporate the effect of measurements into this theory by a stochastic unravelling of the master equation. The resulting equation, in turn, forms the basis for a quantum filter theory along the lines of [14]. The application of the filter approach was so far restricted to systems probed or excited by classical fields, see, e.g., [15–18]. Our stochastic cascaded master equation yields results that are equivalent to the ones obtained in [10] by an alternative method. We believe that the derivation of our master stochastic equation is more straightforward and its application is more readily extended and applied for parameter estimation and hypothesis testing.

We present simple examples of our formalism for the readout of the state of a qubit and for the discrimination between discrete values of its physical interaction parameters. We consider photon counting and homodyne detection of the transmitted field and we supplement our inference among different hypotheses by simulated detection records with the calculation of a deterministic lower limit of the average error by any possible detection scheme on the qubit and the emitted radiation. While our examples deal with the distinction between discrete hypotheses we note that the theory readily applies also to the precision measurement of continuous parameters cf. [18–20].

The article is structured as follows. In Sec. II we introduce the description of the interaction between a quantum pulse and a discrete quantum system. In Sec. III, we model the stochastic dynamical equation of the quantum pulse and the quantum

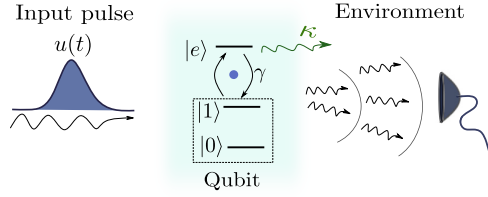*m.khanahmadi@chalmers.se
†klaus.molmer@nbi.ku.dk

FIG. 1. Schematic of qubit state readout by an incoming quantum pulse. The incident light pulse with shape $u(t)$ excites a closed optical transition between the qubit state $|1\rangle$ and excited state $|e\rangle$. The amount of absorption from the pulse and the field correlations induced by the interaction with the qubit system are registered by continuous photon counting or homodyne detection. By introduction of a virtual cavity as the source of the incident pulse, we obtain an effective single-mode open systems treatment of the physical interactions; see text.

system due to the back action of the continuous counting or homodyne measurements. In Sec. IV we present the Baysian inference from simulated signal records about the initial state of a qubit quantum system or a system parameter. In Sec. V we present a lower limit for the average inference error based on the ultimate distinguishability of the candidate quantum states of the qubit and the emitted multimode field. We summarize the results and some theoretical considerations on the applied method in Sec. VI.

II. CASCADED MASTER EQUATION

There is a fundamental difference between the time-dependent interaction of a quantum system traversing a field eigenmode confined in a cavity and the time-dependent interaction of an incident single-mode pulse of traveling radiation with a localized quantum system. In the first case, the field is restricted to discrete eigenmodes and the single-mode Jaynes-Cummings model may apply to an excellent approximation, while in the second case, the field is free to explore a continuum of propagating modes and any nonlinearity in the quantum system thus leads to population of a multimode output field. Quadratic interactions, leading to linear equations for the field amplitudes, were dealt with by input-output theory [21], while scattering of single- and two-photon wave packets on a two-level system was solved by scattering theory [22–25]. However, outside these exceptions, treatments of the interactions between a quantum pulse and a scatterer seem prohibitively complicated due to the dimensionality of the multiphoton and multimode Hilbert space. It has been shown, however, that the theory of cascaded input-output quantum systems [26,27] permits treating the scatterer and a single mode of the radiation field as an open quantum system. This idea was first implemented in [9,10], where effective coupled master equations of the scatterer were associated with each Fock state of the pulse. In this article, we shall adopt a simpler treatment with a virtual cavity that leaks the pulse towards the target, as described by a more conventional cascaded master equation [11,12]. Figure 1 shows a system with two stable levels ($|0\rangle$, $|1\rangle$) and a state $|e\rangle$ that is excited from $|1\rangle$ by the interaction with the incoming pulse with strength $\sqrt{\gamma}$ and decays spontaneously with rate γ. We assume, for simplicity,

that the input and output fields are transversally single mode while populating a continuum of radiation modes propagating from left to right in the figure (chiral coupling).

To obtain a traveling wave packet $u(t)$ as the output from a one-sided quantum cavity with a single-mode annihilation operator a_u, we must assume a time-dependent coupling strength

$$g(t) = \frac{u^*(t)}{\sqrt{1 - \int_0^t dt' |u(t')|^2}}, \quad (1)$$

between the cavity and the input continuum field $b_{\text{in}}(t)$

$$H_{u,\text{cavity}} = i[g^*(t) b_{\text{in}}^\dagger(t) a_u - g(t) b_{\text{in}}(t) a_u^\dagger], \quad (2)$$

where the initial state of the cavity mode can be chosen to represent any Fock state or quantum superposition state of the probe field pulse. In the examples in this article we assume Fock states and coherent states and we assume a Gaussian temporal shape of the pulse

$$u(t) = \frac{1}{\sqrt{\tau} \pi^{\frac{1}{4}}} e^{\frac{-(t-t_m)^2}{2\tau^2}}, \quad (3)$$

with a duration parametrized by τ and a peak occurring at time t_m.

We treat the quantum scatterer by a Hamiltonian H_s and its exchange of quanta with the incident pulse can now be equivalently described as a coupling to the u-cavity mode with the interaction Hamiltonian

$$H_{us} = i\frac{\sqrt{\gamma}}{2}[g_u(t) a_u^\dagger c - g_u^*(t) a_u c^\dagger], \quad (4)$$

where c and $c^\dagger$ are raising and lowering operators of the scatterer by the absorption or emission of a quantum of radiation (in our example, $c = |1\rangle\langle e|$). Radiation propagating to the right of the emitter is composed of the incident pulse (loss by the cavity) and the emission by the quantum scatterer and is described by the coherent lowering operator on these two systems

$$L_0(t) = g_u^*(t) a_u + \sqrt{\gamma}\sigma. \quad (5)$$

Finally, the quantum state of the cavity and the system is described by the density matrix $\varrho_{us}(t)$, which solves the master equation

$$\frac{d\varrho_{us}(t)}{dt} = -i[H, \varrho_{us}(t)] + \sum_{i=0}^n \mathcal{D}[L_i]\varrho_{us}(t), \quad (6)$$

where $H = H_s + H_{us}$ and the Lindblad terms $\mathcal{D}[L_i]\rho = -\frac{1}{2}(L_i^\dagger L_i \rho + \rho L_i^\dagger L_i) + L_i \rho L_i^\dagger$ apply for both L_0 in Eq. (5) and for any additional dissipative local Lindblad operators, $L_i, i = 1, \ldots, n$.

The interference of the two lowering operator terms in the Lindblad operator L_0 is responsible for the cascaded nature of the master equation: Both $D[L_0]\rho$ and the commutator with the interaction Hamiltonian contribute terms of the form $a_u^\dagger c$ ($a_u c^\dagger$), multiplying ρ_{us} from the left (right) in Eq. (6), but these terms cancel each other out and, effectively, no atomic excitation is returned to the source cavity mode.

An exemplary further dissipation mechanism is atomic decay with rate κ by emission into a different, unobserved

direction, see Fig. 1. Such decay is merely represented by one of the separate Lindblad terms in Eq. (6), with

$$L_1 = \sqrt{\kappa} |1\rangle\langle e|. \tag{7}$$

III. QUANTUM TRAJECTORIES FOR THE OBSERVED SYSTEM

We model the conditional dynamics of the system due to measurement of the transmitted field by replacing the deterministic master Eq. (6) by a corresponding stochastic master equation [28,29]. For classical probe fields (coherent states), the cascaded master equation reduces to a stochastic equation that involves only the conditional density matrix for the driven scatterer [12,30], while for other states of the incident probe field we must retain the stochastic evolution of the combined virtual cavity and scatterer system.

A. Counting measurement

We consider first photon counting measurements on the pulse transmitted by the quantum system as depicted in Fig. 1. The stochastic evolution of the density matrix includes a continuous no-jump part for the (unnormalized) density matrix $\tilde{\varrho}(t)$,

$$d\tilde{\varrho}(t) = \left[-i[H, \tilde{\varrho}(t)] + \sum_{i=1}^{n} \mathcal{D}[L_i]\tilde{\varrho}(t) - \frac{1}{2}\{L_0^\dagger L_0, \tilde{\varrho}(t)\} \right] dt \tag{8}$$

and the occasional quantum jump part

$$\tilde{\rho} \rightarrow L_0 \tilde{\varrho}(t) L_0^\dagger, \tag{9}$$

occurring with the probability $\delta p = \langle L_0(t)^\dagger L_0(t)\rangle dt$. Note that the operator averages (and the jump probability) can be obtained only after proper normalization of $\tilde{\varrho}$. A realization of the atomic and field dynamics in an experiment employing photon counting according to Eqs. (8) and (9) is shown in Fig. 2.

B. Homodyne measurement

In homodyne detection, the radiation is mixed on a beam splitter with a strong local oscillator with the same frequency. The difference between the photon flux at the two output-ports yields a noisy and continuous signal dY_t, with a component proportional to, say, the first quadrature of the quantized field represented by L_0 and a white noise term dW_t,

$$dY_t = \text{Tr}(L_0\varrho + \varrho L_0^\dagger)dt + dW_t. \tag{10}$$

dW_t is a Wiener increment with zero mean and variance dt. Note that the mean value of the field quadrature is calculated according to the normalized density matrix ϱ.

The measurement back action of the homodyne detection can be incorporated together with the deterministic evolution in the unnormalized stochastic differential equation

$$d\tilde{\varrho}(t) = \left[-i[H, \tilde{\varrho}(t)] + \sum_{i=0}^{n} \mathcal{D}[L_i]\tilde{\varrho}(t) \right] dt$$
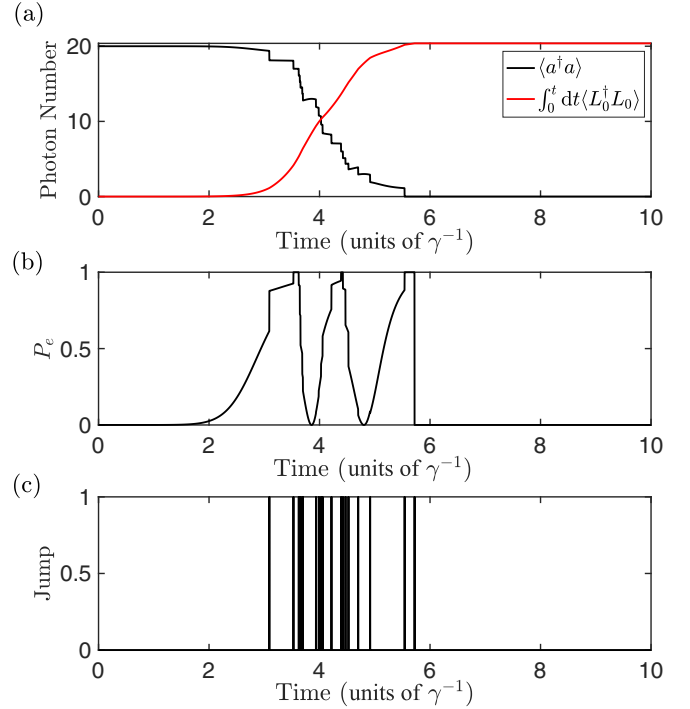$$+ [L_0\tilde{\varrho} + \tilde{\varrho}L_0^\dagger]dY_t. \tag{11}$$

FIG. 2. Single trajectory of an atom initialized in the ground state $|\psi\rangle = |1\rangle$ interacting with an incoming $n = 20$ photon number state pulse, where the output field is subject to unit efficiency photon counting. We assume no further dissipation channels and that all emission is in the forward direction, cf. Fig. 1. Panel (a) shows the mean number of photons in the cavity mode representing the incident Gaussian wave packet (black line) and the integral of the mean photon detection rate (red line). Panel (b) shows the Rabi oscillation-like evolution of the excited state probability P_e of the two-level system. Panel (c) shows the (20) individual photon detection events simulated to occur during the passage of the pulse. The pulse shape is given in Eq. (3) with the parameters $\tau = \gamma^{-1}, t_m = 4\gamma^{-1}$.

A realization of Eq. (11) is shown in Fig. 3.

IV. HYPOTHESIS TESTING

If a system is subject to dynamics according to different candidate physical parameters, we may treat those as a set of hypotheses, $\{h_i, i = 1, \ldots, m\}$, with corresponding prior probabilities $p_0(h_i)$. Given the outcome of measurements, we can use Bayes rule to update the probabilities and infer the most likely among the hypothesis. To this end, the stochastic master equation is solved in parallel for density matrices $\tilde{\rho}_i(t)$ for each candidate hypothesis i. These density matrices directly constitute a Bayesian filter: the probability for a measurement outcome is, for each different hypotheses i, given by $\tilde{\varrho}_i$ via Born's rule. In fact, for a given data record, the relative probabilities of different hypotheses are merely accumulated in the norm of the unnormalized density matrices, $p(D|h_i) \propto \text{Tr}(\tilde{\varrho}_i)$ subject to the stochastic master equation, assuming the measurement outcomes of the record.

According to Bayes rule, it thus follows that the likelihood of the different hypotheses are updated as $p(h_i|D) \propto p(D|h_i)p_0(h_i)$. Henceforth we shall write $p_i = p(h_i|D)$ for the normalized likelihood and we note that the Bayesian update
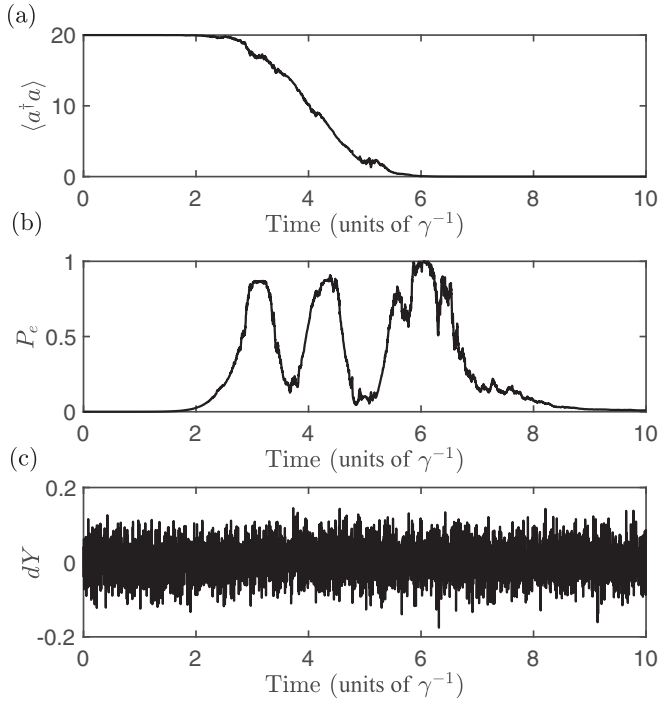
FIG. 3. Single trajectory of an atom initialized in the ground state $|\psi\rangle = |1\rangle$ interacting with an incoming $n = 20$ photon number state pulse, where the output field is subject to homodyne detection. We assume no further dissipation channels and that all emission is in the forward direction, cf. Fig. 1. Panel (a) shows the mean number of photons in the cavity representing the input pulse. Panel (b) shows the excited state population P_e of the atom. Panel (c) shows the stochastic signal (10) obtained during the time interval [0,10]. The pulse shape is given in Eq. (3) with the parameters $\tau = \gamma^{-1}$, $t_m = 4\gamma^{-1}$.
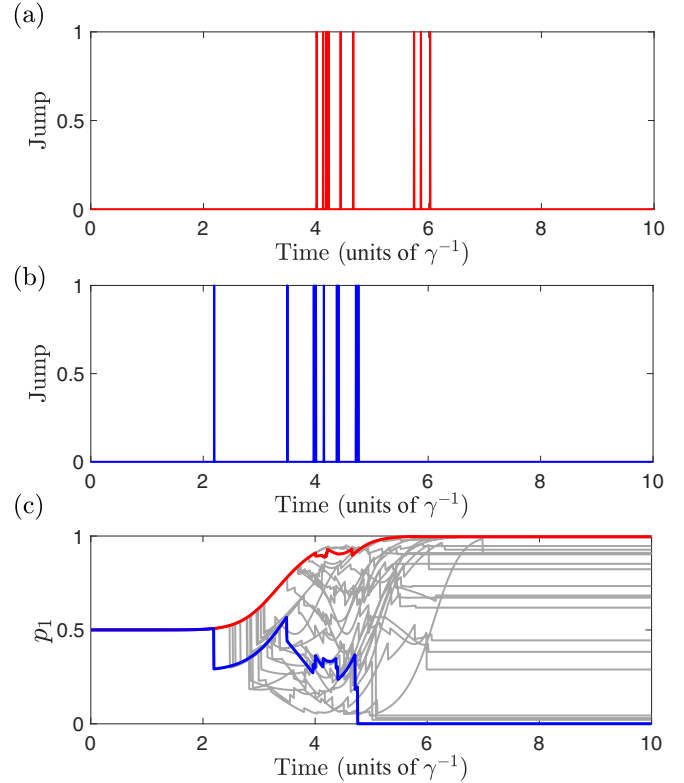

FIG. 4. Two realizations of photon counting signals. Panels (a) and (b) show simulated photon counting signals for a Gaussian pulse prepared in an $|N = 10\rangle$ Fock state, after its interaction with a qubit system prepared in state $|1\rangle$ and $|0\rangle$, respectively. Panel (c) shows the inferred conditional probability that the initial state was $|1\rangle$. The upper solid red and the lower solid blue curves correspond to the simulated detection record in panels (a) and (b), respectively. The gray thin curves are obtained with other detection records, assuming the initial state $|1\rangle$ and $|0\rangle$ with equal probability. The pulse shape is given in Eq. (3) with the parameters $\tau = \gamma^{-1}, t_m = 4\gamma^{-1}$.

may be obtained iteratively over time, cf. the time evolution of the conditional density matrices. The identification of the stochastic master equation with the Bayesian filter [15–18] applies straightforwardly to our quantum pulse master equation and we are hence able to directly assess how the probing with quantum pulses can be employed for different sensing tasks.

A. Qubit state readout

In the following, we shall consider the determination of the state of a qubit in the $\{|0\rangle, |1\rangle\}$ subspace of the atomic system depicted in Fig. 1. We assume that the incident light pulse interacts with the atom on the closed optical transition $|1\rangle \leftrightarrow |e\rangle$ and we shall show that this interaction is revealed in the noisy signal records.

We thus deal with two hypotheses, namely, the two possible initial qubit states $|0\rangle$ and $|1\rangle$, and we assume equal initial probabilities, $p_0(t=0) = p_1(t=0) = 1/2$. The best estimate of the actual initial qubit state at any time during the measurements is the one assigned the highest conditional probability $\max[p_0(t), p_1(t)]$. That choice, however, will be in error with the remaining probability $Q_e = 1 - \max[p_0(t), p_1(t)]$.

Since all incident photons are eventually detected in the output, the total photon count is independent of the state of the qubit, but the temporal distribution of detector clicks and the correlations in the full detection record may still reveal the interaction or not with an effective two-level transition. While these may involve multitime correlations of a very complex character, the strength of the Bayesian quantum trajectory analysis is that it requires no prior knowledge or formal analysis of such correlations. The quantum trajectory itself constitutes a filter that extracts the maximum information from all available data and their temporal correlations in the detection record. Our analysis is readily applicable with more complex investigations, e.g., of interferometric setups and their exploration with general quantum states of light [31,32].

B. Results

Figure 4 shows the outcome of different realizations of the photon counting record for a Gaussian wave packet with ten photons interrogating the three level atom depicted in Fig. 1. Sample detection records are shown in Figs. 4(a) and 4(b) with initial qubit states $|1\rangle$ and $|0\rangle$, respectively.
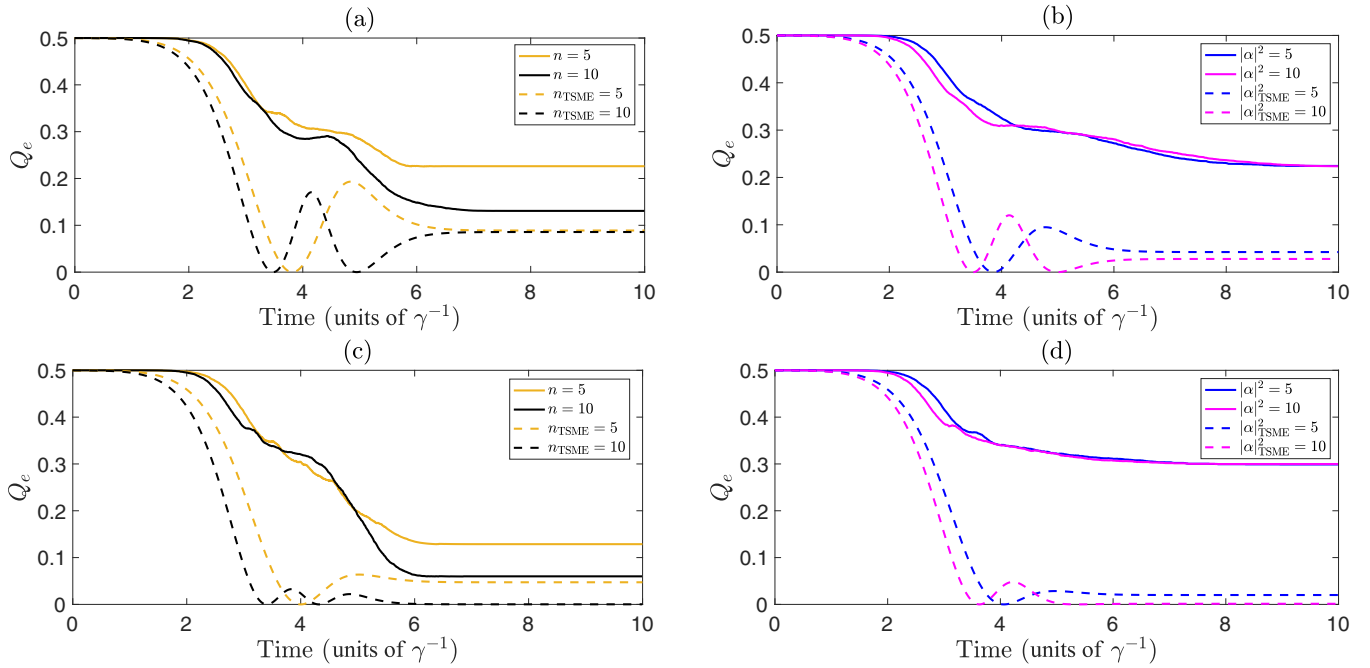
FIG. 5. Comparison of the mean error of the qubit readout with Fock and coherent probe pulses of light. The upper panels of (a) and (b) show the results where the atom only emits in the forward direction while panels (c) and (d) show the results when the excited atoms is subject to an extra decay channel with rate $\kappa = \gamma$. In all panels the solid lines correspond to the Bayesian approach averaged over 1000 simulated trajectories, while the dashed lines refer to the solution of the two-sided master equation (15), which yields a deterministic minimum average error of the parameter estimation; see text. In both left panels (a) and (b), the upper yellow and lower black curves represent Fock states with five and ten photons while in panels (b) and (d), the upper blue and lower purple curves represent coherent states with $\alpha = \sqrt{5}$ and $\sqrt{10}$, respectively. The pulse shape is given in Eq. (3) with the parameters $\tau = \gamma^{-1}, t_m = 4\gamma^{-1}$.

Figure 4(c) shows with solid red and blue curves the inferred, conditional probabilities that the initial state was $|1\rangle$. We see that despite the similarity of the detection records in the upper panels, the inference clearly favors the correct, different initial qubit states. While the total number of detected photons is the same for both hypotheses, their temporal distributions differ as the interaction with the atom can both change the mean intensity profile and the intensity correlations within the pulse. The thin light curves in Fig. 4(c) show how the performance of the qubit readout varies for an ensemble of simulated detection records, chosen with random initial qubit states.

In Fig. 5, we show the average outcome over 1000 simulations of the photon counting detection record (solid lines). To compare how well different input probe states serve to distinguish the qubit state of the atomic scatterer, the figure shows the average probability that the assignment fails (the average error probability) for Fock states with $N = 5$ and 10 photons as well as coherent states $|\alpha\rangle$ with $\alpha = \sqrt{5}$ and $\sqrt{10}$. In Figs. 5(a) and 5(b) we assume that the atom only emits radiation in the forward direction, while in Figs. 5(c) and 5(d) we assume an extra atomic loss process with rate $\kappa = \gamma$. The extra loss is only incurred, if the qubit is in state $|1\rangle$ and hence the initial qubit state is revealed by the detection of a statistically significant reduction in photon number. For the Fock state input [Fig. 5(c)], we thus see a significant reduction in the error probability, while the error is even increased in the case of coherent state probing in Fig. 5(d). The lower dashed curves are discussed in the subsequent section.

V. MINIMUM ERROR IN HYPOTHESIS TESTING

Instead of determining the state of a qubit, the distinction of the detection records may equivalently be employed to infer if a two-level system is coupled to the field with a vanishing or finite coupling strength γ. For that system, these two cases would yield two different time-dependent states $|\psi_0^{\text{all}}(t)\rangle, |\psi_1^{\text{all}}(t)\rangle$, for the combined system of the incident pulse, the two-level scatterer, and the multimode output field environment. An experimentalist with measurement capabilities limited only by the laws of quantum mechanics, may distinguish among such states with a discrimination error

$$Q_e = \frac{1 - \sqrt{1 - |\alpha|^2}}{2}, \quad (12)$$

where $\alpha = \langle \psi_0^{\text{all}} | \psi_1^{\text{all}} \rangle$ is the overlap between the states.

While these states involve unwieldy multimode field-state components after the interaction with the scatterer, their state vector overlap can be easily calculated. Following [33], we assume the same initial incident state of the scatterer and the u mode and we pretend that the interaction strength γ is conditioned on the state of an ancillary control qubit control, prepared in an initial superposition state, so that the combined system evolves into an entangled state

$$|\psi(t)\rangle = \frac{1}{\sqrt{2}} \big[|0\rangle |\psi_0^{\text{all}}(t)\rangle + |1\rangle |\psi_1^{\text{all}}(t)\rangle \big]. \quad (13)$$

Equivalent to the derivation of Eq. (6), it is possible to obtain a cascaded master equation for the reduced state of the ancilla

qubit, the input cavity mode and the two-level scatterer and hence determine the expectation value of the ancilla qubit observable $\langle \sigma^+ \rangle = \langle (|0\rangle\langle 1|) \rangle$. Note from Eq. (13) that this quantity yields half the overlap of the complex scatterer and input and output field states.

The ancilla-dependent system Hamiltonian, Lindblad operators, and density matrix can be represented as block operators in the qubit basis of the ancilla as follows: $H_{\text{total}} = \begin{bmatrix} H_0 & 0 \\ 0 & H_1 \end{bmatrix}$, $L_{\text{total}} = \begin{bmatrix} L_0 & 0 \\ 0 & L_1 \end{bmatrix}$, and $\varrho_{\text{total}} = \frac{1}{2}\begin{bmatrix} \varrho_{00} & \varrho_{01} \\ \varrho_{10} & \varrho_{11} \end{bmatrix}$, respectively. It follows that

$$\alpha(t) = \left\langle \psi_0^{\text{all}}(t) \middle| \psi_1^{\text{all}}(t) \right\rangle = 2\langle \sigma^+ \rangle = \text{Tr}[\varrho_{01}(t)], \qquad (14)$$

where it follows from the master equation that ϱ_{01} solves a two-sided master equation (TSME)

$$\dot{\varrho}_{01} = -i(H_0\varrho_{01} - \varrho_{01}H_1) + L_0\varrho_{01}L_1^\dagger$$
$$- \frac{1}{2}(L_0^\dagger L_0\varrho_{01} - \varrho_{01}L_1^\dagger L_1). \qquad (15)$$

We can readily solve Eq. (15) with the Hamiltonian and Lindblad operators determined in Eqs. (4) and (5) with the two candidate values of γ and the smallest possible value of the estimation error, Eq. (12), achieved by any measurement on the full quantum state, can hence be readily evaluated for all times.

The result of the TSME for different Fock states and coherent states are depicted as the lower dashed curves in Fig. 5. In precision sensing with open quantum systems, photon counting and homodyne detection are sometimes capable of saturating the quantum lower error bounds and thus extract all relevant information about an unknown parameter [18–20]. Here, we see this is not the case. This is chiefly due to the emitter being also part of the full quantum state. At certain moments during the Rabi oscillation dynamics, the emitter coupled to the pulse is predominantly in the excited state and hence perfectly distinguishable from the ground state pertaining to the case of the uncoupled emitter. This yields the occasional vanishing of the error probability, following the Rabi oscillations of the (coupled) system. The simulated error is higher because the state of the emitter is assumed not to be directly available for the photon counting scheme. Recall that we explicitly want to employ the light probe to indirectly perform the qubit readout.

VI. SUMMARY AND DISCUSSION

In this article we presented a general formalism for the interrogation of a quantum system by a quantum probe pulse of radiation. We established the stochastic master equation, which provides the time-dependent state of the probe and the scatterer conditioned on the measurement record (assuming counting or homodyne detection). The master equation readily translates to a filter equation providing conditional probabilities for different hypotheses governing the initial state or parameters in the evolution of the system. We illustrated the stochastic formalism by simulating the detector signal following the interaction between an incoming wave packet and a qubit system, for which our Bayesian filter exhausts the information available in the detection record about the initial qubit state. Our analysis permits the first quantitative assessment of probing of quantum systems with nonclassical multiphoton pulses of light and our simulations confirmed the expectation that Fock probe states may be superior over coherent states for such tasks. Our method readily applies for a much wider class of quantum states and measurement settings, i.e., pulses incident on interferometer setups.

We characterized the achievements of the sensing schemes by averaging the probability of error over many simulated trajectories and we compared our results with a deterministic theory by an extended master equation [33] that yields the minimum error probability Q_e obtained by *any* hypothetical measurement on the scatterer and the emitted field. Such analyses may be supplemented by extended master equation methods like the protocols developed to calculate the (classical and quantum) Fisher information for continuous measurement records in [18,19]. Further studies may guide efforts to optimize probe quantum states and strategies and we suggest this as a promising avenue for future exploration.

Note added. Recently, we became aware of a recent publication studying the limits to precision sensing of atomic interaction parameters with pulses of radiation [34]. The use of one-photon states is studied in detail, including the identification of the optimal detection scheme, while the general pulse method employed in the present article is reviewed and used to confirm the results.

[1] C. M. Caves, Quantum-mechanical noise in an interferometer, Phys. Rev. D **23**, 1693 (1981).

[2] V. Giovannetti, S. Lloyd, and L. Maccone, Advances in quantum metrology, Nat. Photonics **5**, 222 (2011).

[3] S. L. Braunstein and C. M. Caves, Statistical Distance and the Geometry of Quantum States, Phys. Rev. Lett. **72**, 3439 (1994).

[4] W. Pfaff, C. J. Axline, L. D. Burkhart, U. Vool, P. Reinhold, L. Frunzio, L. Jiang, M. H. Devoret, and R. J. Schoelkopf,

Controlled release of multiphoton quantum states from a microwave cavity memory, Nat. Phys. **13**, 882 (2017).

[5] H J. Kimble, The quantum internet, Nature (London) **453**, 1023 (2008).

[6] J. I. Cirac, P. Zoller, H. J. Kimble, and H. Mabuchi, Quantum State Transfer and Entanglement Distribution among Distant Nodes in a Quantum Network, Phys. Rev. Lett. **78**, 3221 (1997).

[7] D. N. Matsukevich and A. Kuzmich, Quantum state transfer between matter and light, Science **306**, 663 (2004).

[8] A. Stute, B. Casabone, B. Brandstätter, K. Friebe, T. E. Northup, and R. Blatt, Quantum-state transfer from an ion to a photon, Nat. Photonics **7**, 219 (2013).

[9] B. Q. Baragiola, R. L. Cook, A. M. Brańczyk, and J. Combes, *n*-photon wave packets interacting with an arbitrary quantum system, Phys. Rev. A **86**, 013811 (2012).

[10] B. Q. Baragiola and J. Combes, Quantum trajectories for propagating fock states, Phys. Rev. A **96**, 023819 (2017).

[11] A. H. Kiilerich and K. Mølmer, Input-Output Theory with Quantum Pulses, Phys. Rev. Lett. **123**, 123604 (2019).

[12] A. H. Kiilerich and K. Mølmer, Quantum interactions with pulses of radiation, Phys. Rev. A **102**, 023717 (2020).

[13] K. A. Fischer, R. Trivedi, V. Ramasesh, I. Siddiqi, and J. Vučković, Scattering into one-dimensional waveguides from a coherently-driven quantum-optical system, Quantum **2**, 69 (2018).

[14] V. P. Belavkin, Quantum filtering of markov signals with white quantum noise, in *Quantum Communications and Measurement* (Springer, 1995), pp 381–391.

[15] J. Gambetta and H. M. Wiseman, State and dynamical parameter estimation for open quantum systems, Phys. Rev. A **64**, 042105 (2001).

[16] B. A. Chase and J. M. Geremia, Single-shot parameter estimation via continuous quantum measurement, Phys. Rev. A **79**, 022314 (2009).

[17] M. Tsang, Continuous Quantum Hypothesis Testing, Phys. Rev. Lett. **108**, 170502 (2012).

[18] S. Gammelmark and K. Mølmer, Bayesian parameter inference from continuously monitored quantum systems, Phys. Rev. A **87**, 032115 (2013).

[19] S. Gammelmark and K. Mølmer, Fisher Information and the Quantum Cramér-Rao Sensitivity Limit of Continuous Measurements, Phys. Rev. Lett. **112**, 170401 (2014).

[20] A. H. Kiilerich and K. Mølmer, Bayesian parameter estimation by continuous homodyne detection, Phys. Rev. A **94**, 032103 (2016).

[21] C. W. Gardiner and M. J. Collett, Input and output in damped quantum systems: Quantum stochastic differential equations and the master equation, Phys. Rev. A **31**, 3761 (1985).

[22] J.-T. Shen and S. Fan, Strongly correlated multiparticle transport in one dimension through a quantum impurity, Phys. Rev. A **76**, 062709 (2007).

[23] D. Witthaut, M. D. Lukin, and A. S. Sørensen, Photon sorters and QND detectors using single photon emitters, Europhys. Lett. **97**, 50007 (2012).

[24] S. Mahmoodian, M. Čepulkovskis, S. Das, P. Lodahl, K. Hammerer, and A. S. Sørensen, Strongly Correlated Photon Transport in Waveguide Quantum Electrodynamics with Weakly Coupled Emitters, Phys. Rev. Lett. **121**, 143601 (2018).

[25] F. Yang, M. M. Lund, T. Pohl, P. Lodahl, and K. Mølmer, Deterministic Photon Sorting in Waveguide QED Systems, Phys. Rev. Lett. **128**, 213603 (2022).

[26] H. J. Carmichael, Quantum Trajectory Theory for Cascaded Open Systems, Phys. Rev. Lett. **70**, 2273 (1993).

[27] C. W. Gardiner, Driving a Quantum System With the Output Field from Another Driven Quantum System, Phys. Rev. Lett. **70**, 2269 (1993).

[28] H. M. Wiseman and G. J. Milburn, *Quantum Measurement and Control* (Cambridge University Press, Cambridge, England, 2009).

[29] K. Jacobs, *Quantum Measurement Theory and its Applications* (Cambridge University Press, Cambridge, England, 2014).

[30] A. Paris-Mandoki, C. Braun, J. Kumlin, C. Tresp, I. Mirgorodskiy, F. Christaller, H. P. Büchler, and S. Hofferberth, Free-Space Quantum Electrodynamics with a Single Rydberg Superatom, Phys. Rev. X **7**, 041010 (2017).

[31] M. J. Holland and K. Burnett, Interferometric Detection of Optical Phase Shifts at the Heisenberg Limit, Phys. Rev. Lett. **71**, 1355 (1993).

[32] P. C. Humphreys, M. Barbieri, A. Datta, and I. A. Walmsley, Quantum Enhanced Multiple Phase Estimation, Phys. Rev. Lett. **111**, 070403 (2013).

[33] K. Mølmer, Hypothesis Testing with Open Quantum Systems, Phys. Rev. Lett. **114**, 040401 (2015).

[34] F. Albarelli, E. Bisketzi, A. Khan, and A. Datta, Fundamental limits of pulsed quantum light spectroscopy of a two-level atom, arXiv:2210.01065.